PHILOSOPHICAL TRANSACTIONS OF THE ROYAL SOCIETY A MATHEMATICAL, PHYSICAL & ENGINEERING SCIENCES

Particle Dispersion in a Vertical round Sudden-Expansion Flow

Y. Hardalupas, A. M. K. P. Taylor and J. H. Whitelaw

Phil. Trans. R. Soc. Lond. A 1992 **341**, 411-442
doi: 10.1098/rsta.1992.0110

Particle dispersion in a vertical round sudden-expansion flow

By Y. Hardalupas, A. M. K. P. Taylor and J. H. Whitelaw

Imperial College of Science, Technology and Medicine, Mechanical Engineering Department, London SW7 2BX, U.K.

Contents

The dispersion of glass beads in an air flow through sudden step expansions in the direction of gravity has been investigated with phase-Doppler anemometry, which provided measurements of the velocity, flux and concentration characteristics. The purpose was to quantify the effect of increasing the air velocity over a factor of 5 for bead diameters of 40 μm and 80 μm and two expansion diameter ratios, 3.33 and 5, and at mass loadings of beads up to 90% of the air mass flow-rate. The results showed that the beads dispersed into the recirculation zone in the lee of the step by interaction with eddies characterized by length and velocity scales of the order of the expansion step height and the downstream area-averaged velocity. Particle dispersion into the recirculation zone was reduced when the bead mean transit time across the recirculation zone was shorter than the bead relaxation time, defined as the time required for a motionless bead suddenly exposed to a constant velocity fluid stream to reach 63% of its surrounding fluid velocity. Also the centrifuging effect, caused by the mean streamline curvature of the recirculation zone, could reduce particle dispersion into the recirculation zone, when its characteristic dimensionless

Phil. Trans. R. Soc. Lond. A (1992) **341**, 411–442
Printed in Great Britain

group was less than unity. Beads, because of their mass, left the recirculation zone by sliding down the wall and past the air reattachment point or near the step, giving rise to bimodal probability distributions of velocity.

1. Introduction

The dispersion of liquid or solid fuel in recirculating flows is of interest in many technological applications, including combustion in industrial burners and in internal combustion engines. The recirculation zone is arranged to enhance the stability of flames in industrial burners and the local concentration of fuel particles influences the combustion efficiency and the flame stability.

Little information exists on how particles disperse around, and in, recirculation zones because of the difficulty in making the necessary measurements. Humphries & Vincent (1976, 1978) have shown that the dispersion of particles in the recirculation zone depends on their ability to follow the mean flow streamlines and the local turbulent motion of the fluid. Li & Tankin (1989) have used visualization and photographic methods to study the droplets dispersed in a recirculation zone. Velocity measurements in two phase recirculating flows have been obtained with laser diagnostics as, for example, in liquid fuelled swirl stabilized burners (Hardalupas *et al.* 1990; McDonell *et al.* 1986), a two-phase annular jet (Hardalupas *et al.* 1986) and a single-sided backward-facing step (Maeda *et al.* 1982; Ruck *et al.* 1988). These studies show that small particles disperse in the recirculation zone, whereas large particles tend to pass through when they are injected inside it or not to disperse at all when they are injected outside it.

Sudden step expansions provide an appropriate configuration for study, because of the simplicity of the geometry and of the extensive information on the flow characteristics of single phase flows past single steps (Bradshaw & Wong 1972; Etheridge & Kemp 1978; Armally *et al.* 1983; Eaton & Johnston 1981), symmetric steps (Abbott & Kline 1962; Cherdron *et al.* 1978) and round sudden expansions (Khezzar & Whitelaw 1986; Gould *et al.* 1990). This study investigates how particles disperse in the recirculation zone formed downstream of an axisymmetric sudden expansion.

(*a*) *Particle dispersion in sudden-expansion flows*

Visual observation of the sudden-expansion flow shows that fewer particles enter the recirculation zone as the air flow-rate is increased, the expansion ratio decreased and the particle size increased. Particles can only enter a recirculation zone by crossing the dividing streamline due to turbulent dispersion, because their initial conditions usually involve trajectories nearly parallel to the flow axis and the mean flow drag results in centrifuging of the particles away from this zone. Observation of the flow shows that it is the largest eddies, of the order of the pipe radius, which contribute most to the dispersion. One of the aims of this study was to quantify particle dispersion in axisymmetric sudden expansions and to present evidence for the importance of the large eddies in this process.

A measure of particle response to the fluid flow is the Stokes number (Yuu *et al.* 1978; Humphries & Vincent, 1978; Hardalupas *et al.* 1989):

$$St = T_f/\tau_b, \tag{1}$$

where T_f is an appropriate mean or turbulent timescale of the fluid flow and τ_b is the

particle response time (Fuchs 1964). If $St \gg 1$, the particle follows the corresponding characteristic timescale of the fluid, while if $St \ll 1$ the particle is not affected. Particle dispersion in the neighbourhood of the recirculation bubble is enhanced by local air turbulence, while particle transit time across the recirculation zone, centrifugal effects due to the curvature of the air streamlines and weight of the particles can reduce particle dispersion and their relative importance depends on the details of the flow. All four effects can be expressed in the form of a Stokes number and to provide a framework for the remainder of the paper, each effect is considered briefly below.

Particle dispersion in the recirculation bubble was quantified by C_r, the particle concentration inside the recirculation zone. As the Stokes number increased from a value much less than 1, our results showed that C_r increased abruptly for $St_e \approx 1$, where this value is based on a timescale characterizing the large eddies defined as

$$T_f = h/U_0, \tag{2}$$

where the lengthscale of the large eddies in a sudden expansion flow is estimated as equal to the step height h and their convection velocity is approximated by the velocity of the fluid averaged over the area of the large tube U_0. The timescale of the larger of the energy containing eddies was used, rather than the customary estimate of l_e/u', where the lengthscale of the eddies $l_e \approx \frac{1}{10}$ h (Tennekes & Lumley 1972) and $u' \approx U_0$, because it resulted in too small a timescale relative to the particle timescale, to be held responsible for particle dispersion in our flow.

Large eddies, either organized or not, have been found experimentally to be the main mechanism for particle dispersion in a variety of free shear flows, as, for example, in plane mixing layer flows (Kobayashi *et al.* 1987; Lazaro & Lacheras 1989; Kamalu *et al.* 1989; Hishida *et al.* 1989) or jet flows (Hardalupas *et al.* 1989; Yuu *et al.* 1978). Their effect has also been confirmed by numerical simulations (Chung & Troutt 1988; Thomas *et al.* 1983; Squires & Eaton 1990). In reattaching flows, many single-phase flow experiments (Kiya & Sasaki 1985; Cherry *et al.* 1984; Bradshaw & Wong 1972; Gutmark & Ho 1983; Bradshaw *et al.* 1964) have shown that large eddies exist in the shear layer generated by vortex shedding from the boundary layer of the upstream pipe flow and that they carry a large fraction of the shear stress of the separated shear layer.

If the particle response time is large relative to the timescale of the mean flow, a relative velocity, U_{slip}, can arise between the particles and the eddies. Thus, if the particle moves faster than the eddies by U_{slip}, the time for particle interaction with the large eddies, equation (2), is reduced by a factor $U_0/(U_0+U_{slip})$. The Stokes number (2), based on the characteristic timescale of the large eddies and the particle relaxation time, $\tau_b = \rho_b d_b^2/18\mu_f$ for the Stokes flow régime, becomes, as shown in Appendix A,

$$St_e = 18(\rho_f/\rho_b)\,(h/d_b)^2(Re_h)^{-1}U_0/(U_0+U_{slip}), \tag{3}$$

where ρ_f and ρ_b are the densities of the fluid and the particles respectively, d_b is the diameter of the particles and Re_h is the step height Reynolds number defined as $Re_h = hU_0/\nu_f$. If the densities of the fluid and the particles are constant, this Stokes number depends on the particle size, the step height and the air flow-rate. For convenience in the interpretation of the results, the interaction of particles with the large eddies was evaluated assuming that U_{slip} was zero. A further aim of this study was to quantify the effect of these parameters on particle dispersion.

The two mean flow parameters, namely the particle transit time across the reattaching length and the centrifugal effect due to the gas mean streamline curvature, impose limitations on particle response to turbulence. If the particle is to respond to air turbulence, its transit time, T_{tr}, over the distance between the nozzle and the mean reattachment point must be longer than the particle response time, τ_b. This effect was quantified by the transit Stokes number,

$$St_{tr} = T_{tr}/\tau_b, \tag{4}$$

where $T_{tr} = Z_r/\frac{1}{2}(U_u + U_r)$ and Z_r is the reattachment length, U_u is the centreline velocity at the exit of the upstream tube and U_r the centreline velocity at a distance Z_r from the nozzle. Linear deceleration across the centreline was assumed in the estimation.

The second mean flow parameter, the centrifuging of the particles away from the recirculation zone due to the mean streamline curvature, acted against the particle dispersion into the recirculation zone. The relative magnitude of the centripetal force to the viscous drag force acting on the particle can be shown to be estimated by the 'centrifuge' Stokes number, defined as (see, for example, Kriebel 1961; Dring & Suo 1978)

$$St_\omega = 18\mu_f/\rho_b\,\omega d_b^2, \tag{5}$$

where ρ_b and d_b are the density and the diameter of the particle and ω and μ_f are representative values of the angular velocity and viscosity of air, respectively.

Summarizing the effect of the above parameters, this work will show the extent to which the above parameters control particle dispersion in the recirculation zone. First, both Stokes numbers based on the mean flow parameters must be more than 1, namely $St_{tr} > 1$ and $St_\omega > 1$, before particles can disperse in the recirculation zone. Then the particles must respond to turbulent flow to disperse, so the large eddies Stokes number, St_e, must also be larger than one and, as a consequence, the slip velocity relative to the large eddies is important. Once particles have entered the recirculation zone and their mean velocity is small, the fourth parameter, namely their weight, can influence particle dispersion and is evaluated. The presence of the particles in the flow can affect the characteristics of the fluid flow when the mass loading, defined as the mass flow-rate of the particles divided by the mass flow-rate of the air, is larger than at least 15% and the effect of particle mass loading on the fluid flow and on particle dispersion was also examined.

Figure 1 summarizes the mechanisms of particle dispersion due to the large eddies, as indicated by our results, and is discussed in detail later in the text. Trajectories denoted by 1 are particles that attain a small radial velocity component v_b' after their interaction with a large eddy but, because of their initial momentum and inertia, continue to move in straight trajectories till their next interaction with a large eddy. If they reach the wall, they do so with large axial component of velocity. In contrast, those particles which leave the upstream pipe boundary layer with low velocity follow a large eddy for a longer time before being flung out (Kamalu *et al.* 1989) and the result is denoted as trajectory 2. Particles which find themselves in the region of reverse mean flow can be transported towards the step by the reverse mean flow and, depending on their response to the accompanying turbulence, leave the recirculation zone close to reattachment (trajectories 3) or reach the step (trajectories 4) and either are caught by the corner vortex or leave the recirculation zone there. However, it will be shown that most of the particles leave the recirculation zone close to reattachment by sliding on the wall because of their weight. Superposition of trajectories 1 and 2

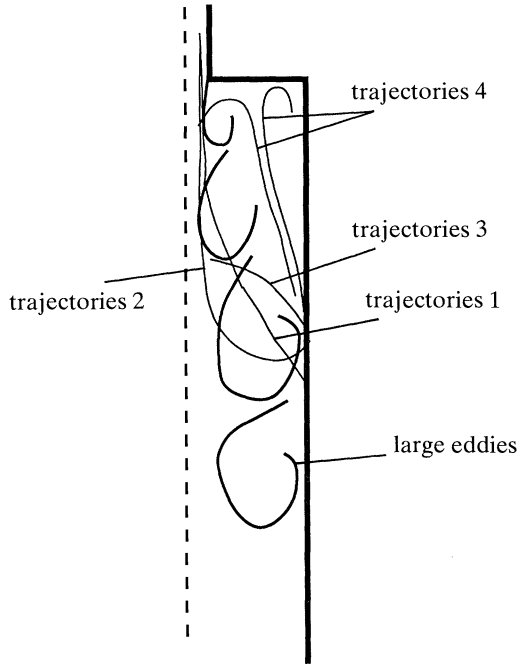

Figure 1. Sketch showing the way the beads disperse into the recirculation zone.

and trajectories 3 and 4 at the same point in the flow but at different instants in time result in bimodal axial velocity probability distribution functions of particles in the neighbourhood of the gas separation streamline.

(*b*) *Outline of the present work*

The present study investigates the dispersion of quasi-monodisperse glass beads in an air flow through sudden step expansions with diameter ratios of 3.33 and 5. The air flowrate was 150 $dm^3\ min^{-1}$ to 700 $dm^3\ min^{-1}$ and the bead sizes 40 μm and 80 μm resulting in a range of large eddies Stokes numbers between 0.1 and 5. Phase Doppler velocimetry yielded values of axial, radial and azimuthal velocity, axial flux and concentration of the glass beads at mass loadings varying from around 15% to 90% as well as the axial velocity of the gas phase in the presence of the beads. The results focus on five aims. Quantification of particle concentration in the recirculation zone, establishing where the particles enter and leave the recirculation zone, assessment of the relative importance of the transit time of particles across the reattachment length, centrifuging and gravity, evaluation of the effect of mass loading on dispersion and provision of evidence of the influence of the large eddies.

Section 2 describes the flow arrangement, the experimental technique and the estimates of measurement uncertainties. Section 3 presents and analyses the results for expansion ratios of 3.33 and 5. The results are summarized and discussed relative to other work in §4. In the following text, *mass loading* is defined as the ratio of the mass flow-rate of the beads to the mass flowrate of the gas. The term *beads* is reserved for the glass beads (subscript b) and *seed* and *seeding* for the seeding material used for the measurement of the gas phase with the phase Doppler anemometer. The term *single phase* refers to the air flow without any beads added (subscript s) and *gas* or *fluid* flow to the motion of the air in the presence of the beads (subscript f). It is

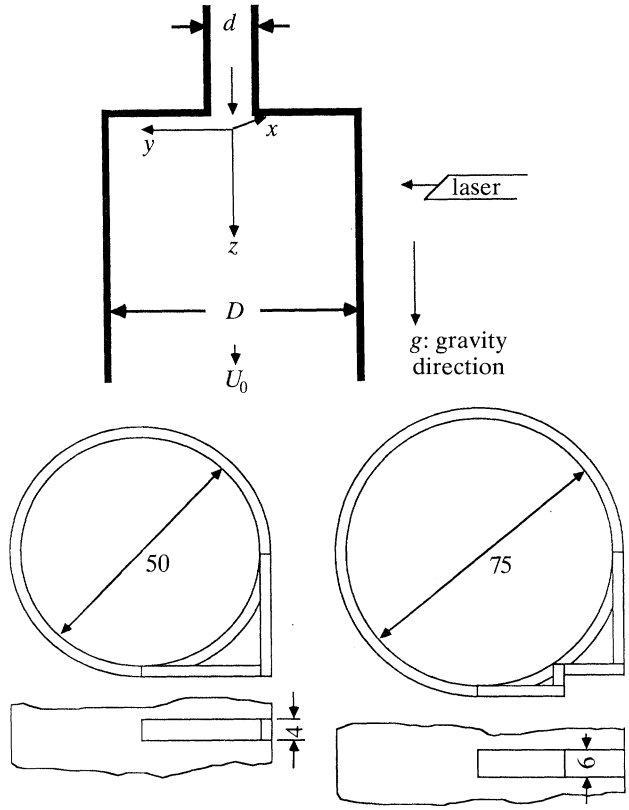

Figure 2. Dimensions of the sudden expansion and coordinate system used.

expected that the velocities measured in the single phase flow are a good approximation to the air flow at low mass loadings of the beads and therefore the single phase is frequently used as a reference.

2. Experimental arrangement

(a) *Flow arrangement*

The experimental arrangement used the bead delivery and recovery arrangements described in detail by Hardalupas *et al.* (1989). The air was supplied by a central compressor and was metered by rotameters to provide pneumatic transport for the glass beads and for the seeding tracer necessary for the measurement of the air velocity. The two streams were recombined upstream of a smooth contraction with 11.1 area ratio and subsequently developed in a 15 mm diameter precision bore stainless steel tube for 100 diameters exhausting vertically downwards and passing over the round sudden step expansion produced by coaxial precision bore glass tubes with internal diameters of either 50 mm or 75 mm at the exit of the steel tube. Details of the geometry are shown in figure 2. The rotameters operated at gauge pressures between 0.1 and 0.3 and the flow rates were corrected to N.T.P. from calibration charts provided by the manufacturer. The minimum air flow-rate was 150 $dm^3\ min^{-1}$, a compromise between the need for large mean Stokes number in the upstream pipe,

Table 1. *Flow conditions*

expansion ratio	3.33		5	
	40 μm	80 μm	40 μm	80 μm
flow rate (dm^3 min^{-1})	140	150	150	150
diameters (mm)				
upstream tube, d	15	15	15	15
expansion tube, D	50	50	75	75
bulk velocity (m s^{-1})				
upstream tube, U_{0i}	13.2	14.2	14.2	14.2
expansion tube, U_0	1.19	1.27	0.57	0.57
Reynolds number				
upstream tube[a]	13000	14000	14000	14000
expansion tube[b]	3900	4200	2809	2809
step height, h[c]	15200	16400	28000	28000

[a] $Re = U_{0i}d/\nu$, [b] $Re = U_0 D/\nu$, [c] $Re = U_{0i}h/\nu$.

and for a Reynolds number based on the step height and the bulk velocity in the upstream pipe higher than 6000 to ensure turbulent flow downstream of the step (Armaly *et al.* 1983), and resulted in an exit Reynolds number of the upstream pipe around 14000, corresponding to the flow conditions given in table 1. The air flowrate was increased up to 700 dm^3 min^{-1} during the experiments to check its effect on bead dispersion.

The precision bore glass tubes facilitated optical access, but the seeding powder used for the gas phase measurements eventually built up on the glass wall, resulting in attenuation of the laser beams. The tube was treated regularly with a proprietary antistatic cleaner, which helped to keep the tube clean for long periods. Electrostatic attraction of the glass beads was not observed. The correlation $\overline{uv}$ was measured by rotating the plane of the laser beams by $\pm 45°$ (Melling & Whitelaw 1975). This required replacement of a part of cylindrical surface of the large tube by flat windows, as shown in figure 2.

The glass beads were supplied to the flow and metered by the screw feeder described by Hardalupas *et al.* (1989). The transport air through the screw feeder box was maintained even when no beads were added, to minimize any disturbance of the operating conditions. The flow was seeded with kaolin, which was nominally micrometre-size before agglomeration, and dispensed by a reverse cyclone feeder (Glass & Kennedy 1977). The flow rate through the reverse cyclone was maintained even when seeding power was not introduced, by using a second reverse-cyclone which had no seed inside it, to ensure that the pressure drop through the system was the same with and without beads. The seeded air flow was directed against the falling beads to promote the radial dispersion of the beads before arriving at the contraction. The seeded air and the beads discharged from the glass tube into a collection hopper driven by the induced draught provided by a large fan. The beads were recovered by passing the flow through a cyclone placed upstream of the fan and returned to the hopper of the screwfeeder.

The size ranges of the beads were 37–44 μm and 60–95 μm (table 2) and will be referred to as 40 μm and 80 μm for convenience. The nominal 40 μm range represents the smallest narrow-sized range that could be found at acceptable cost. The avoidance of problems associated with the surface quality of the beads, their

Table 2. *Nominal properties of glass beads*

	40 μm[a]	80 μm[b]
nominal diameter range/μm	37–44[c]	60–95[d]
density, ρ_b/(kg m^{-3})	2420	2950
stokesian time constant/ms	11.9	47.6
terminal velocity/(cm s^{-1})[e]	11.1	44.8
time constant[f]	11.1	45.7
refractive index	1.51	1.6

[a] Ferro Corporation, Jackson, Mississippi 39205, U.S.A.
[b] Jencons (Scientific) Ltd, Leighton Buzzard, Beds., LU7 8UA, U.K.
[c] Class V, close sized uni-spheres. 90% within size range; 90% true spheres; < 2% irregularly shaped beads.
[d] Grade 15. 20% normally outside 42–102 μm.
[e] Based on table 5 in Fuchs (1964, p. 32).
[f] Based on terminal velocity, τ_b/ms.

sphericity and with the percentage of the number of sizes smaller than the nominal range in the batch encountered during the experiments, is described in detail in Hardalupas *et al.* (1988, 1989), Hardalupas (1989) and Mostafa *et al.* (1987). The mass loading of the beads was varied from around 15% to 90% for both sizes. At the lowest mass loading, the effect of the presence of the particles on the gas flow was negligible. The value of the maximum loading was limited by the need to have no more than one bead in the probe volume of the phase Doppler velocimeter at any instant and by the maximum permissible attenuation of the incident laser beams.

(*b*) *Phase-Doppler anemometer*

A custom built phase-Doppler instrument (Hardalupas 1989) was used with the characteristics of the transmitting optics given in the top portion of table 3; a high power laser gave adequate signal-to-noise ratio for the seeding powder, and frequency shifting was provided by rotation of a radial diffraction grating. The receiving optics were placed at 30° to the forward scatter direction and the associated characteristics are given in the lower portion of table 3, together with the possible size range at each optical setting. Note that the length of the beam intersection volume is determined by the spatial filter of the receiving optics and is much smaller than the intersection volume of the beams. Signals with phase shifts in the interval 0°–40° were accepted as being generated by the seeding powder. The radial and azimuthal mean and root mean square (RMS) velocities were measured by aligning the sensitivity vector of the anemometer at 90° to the axis of the tube. Two different optical arrangements were used and are indicated as systems 1 and 2 in table 3. System 1 was used during the measurement of the axial mean and RMS velocity, whereas system 2 was used for the radial and azimuthal velocity, the flux and the concentration measurements, depending on what was available each time.

The electronic system recorded simultaneous values of velocity and size, interdata arrival time and residence time of each bead in the probe volume and provided information of the flux and number density using the method of Hardalupas & Taylor (1989). The mass flux, G (kg m^{-1} s^{-1}), is given by

$$G = \frac{\rho_b \pi d_b^3}{6 A T_s} \sum_{i=1}^{N} \frac{U_i}{|U_i|}, \tag{6}$$

PHILOSOPHICAL TRANSACTIONS OF THE ROYAL SOCIETY A MATHEMATICAL, PHYSICAL & ENGINEERING SCIENCES

Table 3. *Principal characteristics of the phase-Doppler anemometer*

	system 1	system 2
1 Watt (nominal) Ar^+ laser wavelength/nm	514.5	514.5
laser power/mW	300	80–100
beam diameter, at e^{-2} intensity, of laser/mm	1.25	1.25
focal length of lenses:		
imaging lens from laser to grating/mm	80	100
collimating lens after grating/mm	300	300
imaging lens to form measuring volume/mm	300	600
number of lines on radial diffraction grating	8192	16384
shift frequency (nominal) due to rotation of grating/MHz	3	3
short-term stability of shift frequency (RMS) (%)	0.3	0.3
beam separation/mm	27.7	55.4
measured half-angle of intersection/deg	2.64	2.45
calculated dimensions of beam intersection volume at e^{-2} intensity/mm	1.13	2.45
	0.052	0.105
	0.052	0.105
fringe spacing/mm	5.58	6.018
calculated number of fringes within e^{-2} intensity	8	17
frequency to velocity conversion factor/(MHz ms^{-1})	0.18	0.166
location of collection optics from forward scatter/deg	30	30
focal length of collimating lens in receiving optics module/mm	600	600
apertures at collimating lens:		
dimension of rectangular apertures/mm	45×6	45×6
separation between apertures 1 and 2/mm	25	25
separation between apertures 1 and 3/mm	50	50
focal length of imaging lens in receiving optics module/mm	300	300
width of spatial filter before the photomultipliers/μm	100	100
magnification of receiving optics	2	2
hence effective length of measuring volume/μm	200	200
phase angle-to-diameter conversion factor for channel 1 and 3/(μm deg^{-1})	0.263	0.319

where ρ_b is the density of the beads, N is the total number of the monodisperse beads measured during the sampling time T_s, d_b is the diameter of the beads and A is the effective area of the probe volume. The summation term provides the sign of the velocity and hence the direction of the flux. In the following results, the positive direction is reserved for the movement of the beads away from upstream pipe for the axial component of bead flux.

The concentration C (kg m^{-3}) of the monodisperse beads is evaluated by

$$C = \tfrac{1}{6}\rho_b \pi d_b^3 \frac{\Sigma \tau_i}{T_s} \frac{1}{V}, \tag{7}$$

where τ_i is the residence time of sample i in the probe volume and the ratio $\Sigma\tau_i/T_s$ is the fraction of time that beads are resident in the effective volume V of the probe volume (Hardalupas & Taylor 1989).

(*c*) *Uncertainties*

The uncertainties involved in the measurement of the beads and the gas in the presence of the dispersed phase have been analysed elsewhere (Hardalupas *et al.* 1988, 1989) and table 4 gives the systematic and random errors. The largest

Table 4. *Estimates of systematic and random errors in quantities measured*

quantity	systematic error	random error
position	1 mm	±1 mm
mass loading of beads	—	5%
bulk gas velocity	—	3%
gas phase in presence of beads		
mean velocity	3–4% (towards U_b)	—
RMS velocity	+5 to +10%	—
beads and single phase flow		
mean velocity	+3%	1%
axial RMS velocity	−3%	3%
radial RMS velocity	−5%	5%
cross-correlation	−4%	4%
cross-correlation coefficient	7%	6%
bead flux and concentration	—	30%

contributor to the random error was the population size of the data, typically, 3000 measurements, which result in uncertainties (Yanta & Smith 1978) of 1% and 3% of the axial mean and RMS of velocity of the beads respectively.

The major source of uncertainty in the measurement of gas phase velocities is that some non-spherical or optically imperfect glass beads are erroneously identified as seeding. This problem is addressed in detail by Hardalupas *et al.* (1988) and a cross talk of about 7% of all the beads with an aerodynamic diameter between 35 μm and 45 μm beads was found to exist on the gas phase measurement and this figure was taken as representative for all the bead sizes used. The strategy suggested by Hardalupas *et al.* (1988, 1989) to reduce the effect of cross-talk in the gas phase measurements, resulted in uncertainties in U_f and u'_f due to cross-talk from the large beads of about 3% and 5% of the quoted values respectively.

The measurements of flux and concentration of the beads were made by measuring the data rate, keeping the laser power low enough to avoid detecting signals from bead diameters smaller than the nominal values and assuming that the measurements were all due to beads of the nominal diameter. The sizing validation criteria (Hardalupas 1989) of the instrument were disabled to avoid the rejection of signals from optically imperfect glass beads. The main sources of uncertainties in the measurement of the flux and concentration of the beads were due to fringe count limitations and Hardalupas *et al.* (1991) explained that the large errors in the measurements of axial flux close to the wall for high bead mass loadings are caused by the high beam attenuation. This effect resulted in obviously wrong measurements, since axial fluxes as large as 300 G_0 were measured on the wall, where G_0 is the bead flux averaged over the area of the expansion tube. It should be noted that the erroneously detected large axial flux on the wall resulted in over estimation of the mass flowrate of the beads and hence our results did not conserve bead mass flux. Away from the wall of the tube, the uncertainties of the measured bead flux and concentration were around 30% and this is similar to other estimates in the literature (Dodge *et al.* 1987; Saffman 1987).

3. Results

Results for both expansion ratios and for the 40 μm and 80 μm beads are presented in the following order. Section 3*a* compares the separation streamline of the single phase flow and the zero axial velocity contours of the beads and the gas phase for the two expansion ratios; §3*b* quantifies the influence of increasing air flow-rate on the dispersion of the 40 μm beads in both expansion ratios; §3*c* quantifies the influence of increasing bead size and the step height on bead dispersion; §3*d* examines the effects of the mean flow parameters and gravity on bead dispersion; §3*e* discusses the effect of increasing mass loading on the gas flow and on bead dispersion; and §3*f* presents the effect of the large eddies on the bead motion by examining their velocity characteristics.

The air velocity, U_0, averaged over the area of the expansion tube, was chosen to normalise the velocity profiles and the bead flux, G_0, averaged over the area of the large tube, to normalize the flux measurements. The normalization parameters for the two expansion ratios are summarized in tables 5 and 6 as functions of air flow-rate and in tables 7 and 8 for the air flowrate of around 150 $dm^3\ min^{-1}$. The density of the glass beads, ρ_b, given in table 2 (e.g. 2420 $kg\ m^{-3}$ for the 40 μm beads), was used to normalize the bead concentration results. The diameter of the downstream tube, D, was used to normalize the radial and the axial coordinates of the flow. Cartesian axes with corresponding velocity components were used and the position of the laser relative to these is defined in figure 2, so that the likely effects of light attenuation can be estimated.

(*a*) *Separation streamlines and zero axial velocity loci*

This section provides an overview of the flow. The locus of zero axial velocity for the 40 μm and 80 μm beads and the separation streamline for the single phase flow, as well as the loci of the zero axial velocity for the gas phase in the presence of 80 μm beads, are compared for the lower air flow-rate (around 150 $cm^3\ min^{-1}$). The terms recirculation zone of the beads and reattachment of the beads are used arbitrarily in the rest of the text to refer to the region of the flow enclosed between the locus of the zero bead axial velocity and the wall of the large tube and the locus of the zero bead axial velocity on the wall of the large tube respectively. Although there is no physical meaning associated with these definitions, they can still indicate the region of the flow where there is strong influence of the drag forces imposed by the gas on the trajectories of the beads.

Figures 3 and 4 show the zero mean axial velocity loci of the 40 μm and 80 μm beads for the two expansion ratios and the loci of zero axial velocity of the single phase and the gas phase in the presence of the 80 μm beads for the three mass loadings. The recirculation zone of the 40 μm beads was longer than that of the single phase by 15%, 36% and 57% for the expansion ratio of 3.33 and 13%, 23% and 50% for the expansion ratio of 5 respectively for 13%, 40% and 80% mass loading. In contrast, the recirculation zone of the 80 μm beads in the larger expansion ratio was *shorter* than that of the single phase by 20% and 10% for the 23% and 40% mass loadings respectively and the same for the 86% mass loading. This suggests that the streaklines of the 80 μm beads had smaller radius of curvature than those of the air flow, despite the argument of §1*a* that centrifuging, caused by the curvature of the mean separation streamline, should preclude this possibility. This observation stems from the effect of gravity and the partial response of the beads to

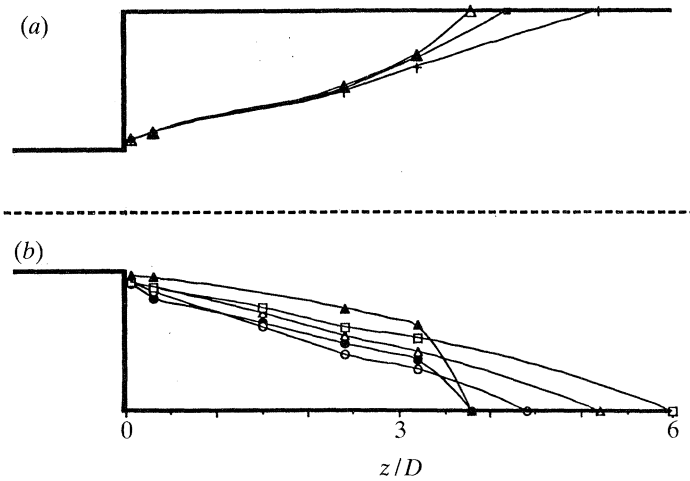

Figure 3. Zero velocity contours. (*b*) The single phase (●), the 40 μm beads for mass loadings of 13% (○), 40% (△) and 80% (□). (*a*) The gas phase in the presence of the 80 μm beads for mass loadings of 23% (△), 40% (■) and 86% (+); and the single phase separation streamline (▲) in the expansion ratio of 3.33.

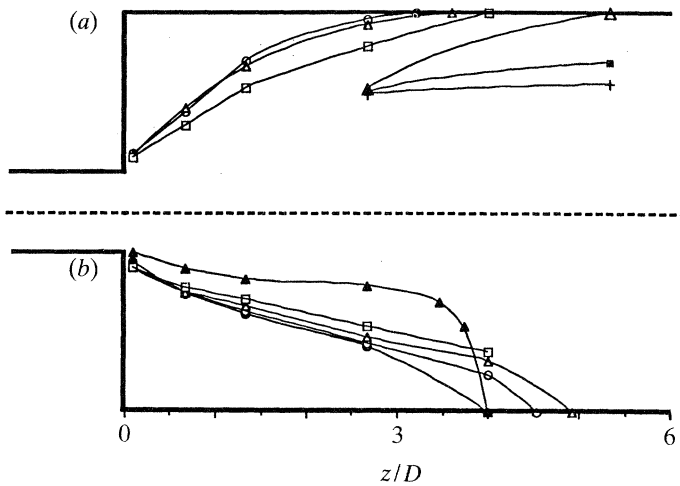

Figure 4. Zero velocity contours. (*b*) The single phase (●), the 40 μm beads for mass loadings of 13% (○), 40% (△) and 80% (□). (*a*) The gas phase in the presence of the 80 μm beads for mass loadings of 23% (△), 40% (■) and 86% (+); and 80 μm beads for mass loadings of 23% (○), 40% (△) and 80% (□); and the single phase separation streamline (▲) in the expansion ratio of 5.

the large eddies and is examined later. The results show that, although the exit mean flow Stokes number of the upstream tube (Hardalupas *et al.* 1989) suggested that all beads should be unresponsive to the mean flow, the 40 μm beads were responsive to the gas recirculation zone for both expansion ratios and that the 80 μm were semi-responsive, since they entered the recirculation zone only for the larger expansion ratio.

The gas phase recirculation zone in the presence of the 80 μm beads was longer than for the single phase flow for all three mass loadings by more than 33% for the expansion ratio of 5 and between 10% and 40% for that of 3.33, because of the momentum transfer from the beads to the gas phase at the central region of the flow.

PHILOSOPHICAL TRANSACTIONS OF THE ROYAL SOCIETY A MATHEMATICAL, PHYSICAL & ENGINEERING SCIENCES

Table 5. *Variation of the air flow-rate in expansion ratio of* 3.33 *in the presence of the* 40 μm *beads*

airflow-rate ($dm^3\ min^{-1}$)	air bulk velocity, U_0 ($m\ s^{-1}$)	G_0/($kg\ m^{-2}\ s^{-1}$)	St_ω	St_{tr}	St_e
150	1.27	0.19	7.4	1.9	1.14
200	1.70	0.27	5.9	1.4	0.86
266	2.26	0.33	4.7	1.0	0.65
325	2.76	0.40	3.9	0.7	0.53
395	3.35	0.45	3.3	0.6	0.43
450	3.82	0.53	2.9	0.5	0.38
525	4.46	0.60	2.6	0.4	0.33

Table 6. *Variation of the air flow-rate in expansion ratio of* 5 *in the presence of the* 40 μm *beads*

air flow-rate ($dm^3\ min^{-1}$)	air bulk velocity, U_0 ($m\ s^{-1}$)	G_0/($kg\ m^{-2}\ s^{-1}$)	St_ω	St_{tr}	St_e
150	0.57	0.09	11.4	3.3	4.41
266	1.00	0.14	6.8	2.0	2.49
395	1.49	0.20	4.8	1.2	1.68
525	1.98	0.27	3.7	0.9	1.26
585	2.21	0.29	3.2	0.8	1.13
645	2.43	0.32	2.9	0.7	1.03
710	2.68	0.34	2.7	0.6	0.93

The effect of the modification of the gas phase flow field by the beads on their dispersion is examined in §3*e*.

Confidence in the accuracy of our measurements was provided by the integration of the air velocity profiles, which yielded volume flow-rates well within 15% of these measured by the rotameters, mainly due to the uncertainty involved in the integration close to the wall. Asymmetries of the mean reattachment length of the order of 15% were found on opposite sides of the tube which is comparable to other experiments (see, for example, Cherdron *et al.* 1978). The reattachment length was measured by placing the laser Doppler probe volume as close to the wall as possible and traversing it in the axial direction till the mean axial velocity changed sign.

(*b*) *Influence of the air flow-rate on the dispersion of the* 40 μm *beads*

Measurements of bead concentration were taken in the axial direction close to the wall, at $y/D \approx 0.50$ and at $y/D = 0.34$. The mass loading of the beads was kept constant at 14% by increasing the mass flow-rate of the beads in proportion to the air flow-rate. The flow conditions and the parameters used for normalization of the results are summarized in tables 5 and 6 for the two expansion ratios. Measurements with the 80 μm beads are not reported, since the beads entered the recirculation zone only at the lowest air flow-rate with the larger expansion ratio. The large eddies Stokes number, St_e (equation (3)), is inversely proportional to the air flow-rate and is used as the parameter in the figures below. The influence of the term $U_0/(U_0+U_{slip})$ on the St_e was assumed negligibly small in the estimates presented in tables 5 and 6, although it can be argued that it is significant for the larger air flow-rates and it will

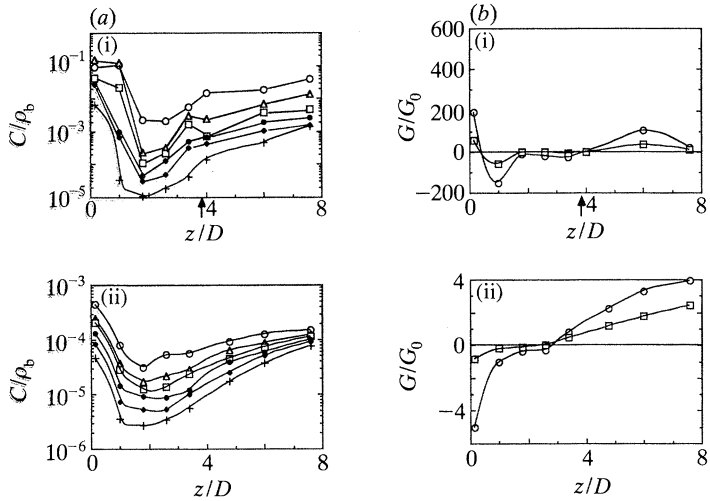

Figure 5. (*a*) Concentration and (*b*) axial flux of the 40 μm beads at (i) $y/D \approx 0.5$ (wall) and (ii) $y/D = 0.34$ in the expansion ratio of 3.33 as a function of the large eddies Stokes number, which was modified by varying the air flow-rate. The arrows indicate the reattachment point of the single phase flow. Large eddie Stokes numbers: ○, 1.14; △, 0.86; □, 0.65; ●, 0.53; ◆, 0.43; +, 0.33.

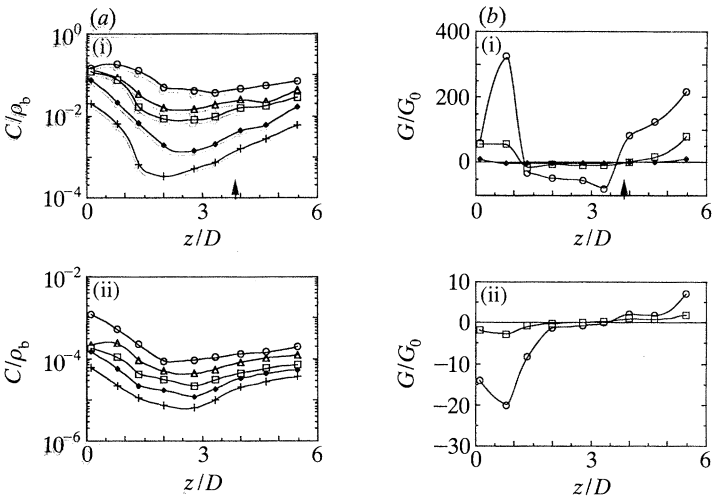

Figure 6. (*a*) Concentration and (*b*) axial flux of the 40 μm beads at (i) $y/D \approx 0.5$ (wall) and (ii) $y/D = 0.34$ in the expansion ratio of 5 as a function of the large eddies Stokes number, which was modified by varying the air flow-rate. The arrows indicate the reattachment point of the single phase flow. Large eddies Stokes numbers ○, 4.41; △, 2.49; □, 1.68; ◆, 1.26; +, 0.93.

lead to smaller values than those presented in tables 5 and 6, but this effect is not going to affect our conclusions.

The concentration profiles of the 40 μm beads along the reattachment length for the two expansion ratios at $y/D \approx 0.5$ and 0.34, figures 5*a* and 6*a*, show that a large change of the bead concentration inside the recirculation zone occurs for a critical value of large eddies Stokes number, St_e, of the order of unity and decreases by a factor of 100 for a decrease of St_e by around 5 and 3 times in the large and the small expansion ratios respectively. This result supports the response of the beads mainly

PHILOSOPHICAL TRANSACTIONS OF THE ROYAL SOCIETY A MATHEMATICAL, PHYSICAL & ENGINEERING SCIENCES

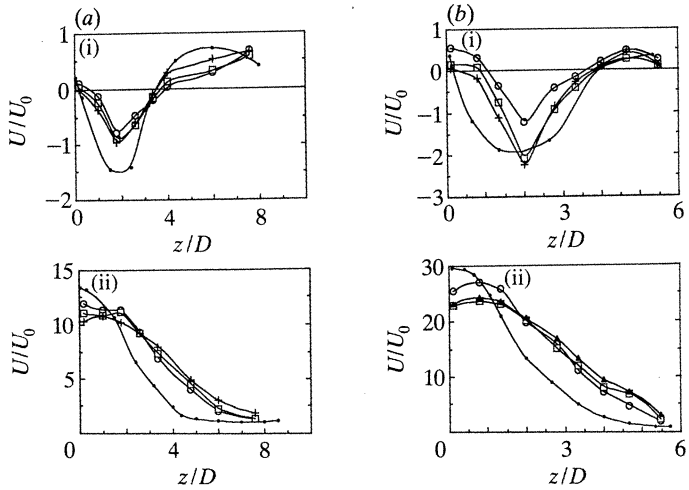

Figure 7. Mean axial velocity of the 40 μm beads at (i) $y/D \approx 0.5$ (wall) and at (ii) the centreline in the (*a*) expansion ratio of 5 and (*b*) expansion ratio of 3.33 as a function of the large eddies Stokes number, which was modified by varying the air flow-rate. The large eddies Stokes number for (*a*): ○, 1.14; □, 0.65; +, 0.33; ●, single phase. For (*b*): ○, 4.41; □, 1.68; +, 0.93; ▲, 1.03; ●, single phase.

to the large eddies of the shear layer close to reattachment (Crowe *et al.* 1985). The arrows on the figures indicate the reattachment length. The wall concentration for a given St_e is far larger than at any other region inside the recirculation zone and the concentration is smaller about half way along the recirculation zone, caused by the centrifuging of the beads by the mean flow field and by the large eddies inside the recirculation.

The concentration and the axial flux profiles of the 40 μm beads, figures 5 and 6, in both expansion ratios show how the beads disperse inside the recirculation zone. The axial bead flux close to the wall and within $\frac{1}{2}D$ from the step is in the positive Z direction and the concentration profiles there have maxima, where the trapped corner vortex exists (figure 7) and centrifuges the beads on the wall and away from the step. On the wall, between $Z \approx \frac{1}{2}D$ and reattachment, the axial flux is directed towards the step and the concentration has minima between these two points which shows that beads disperse backwards from reattachment into the recirculation zone, due to the mean gas flow. Close to reattachment, the figures show that the axial flux of the beads near the wall is positive implying that beads leave the air recirculation zone there mainly by sliding down the wall due to their weight. The concentration increased with downstream distance and air flow-rate, since increasing air flow-rate results in progressively fewer beads entering the recirculation zone and so most of them reach the wall downstream of the recirculation zone.

The mean axial velocity distributions close to the wall, figure 7, show that the reattachment length of the air does not change with the air flowrate, while the locu of the zero axial velocity point of the 40 μm beads on the wall decreased from aroun $z/D = 4$ to 3.5 for the smaller expansion ratio and increased by a similar amount fo the larger expansion ratio by increasing the air flowrate. Comparison between figur 7*a* and 5*b* for the smaller expansion ratio and figures 7*b* and 6*b* for the larg expansion ratio shows that the locus of the zero axial velocity and the zero axial fl do not coincide. Also the locus of zero axial flux suggests that the reattachm length of the beads increased for both expansion ratios with the increase of the

Figure 8

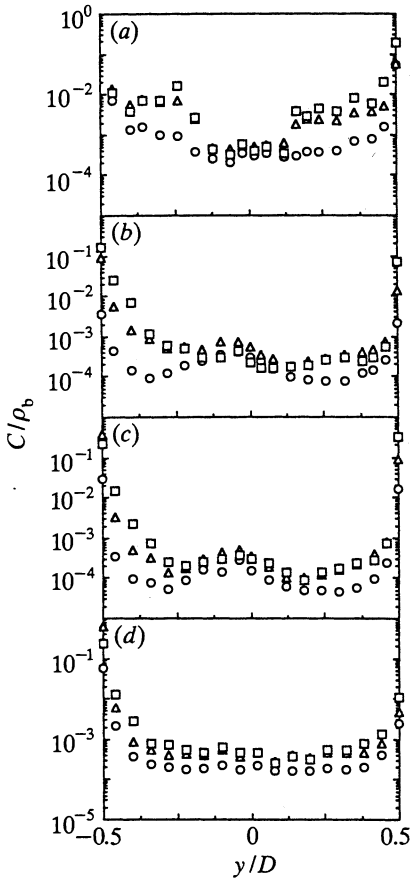

Figure 9

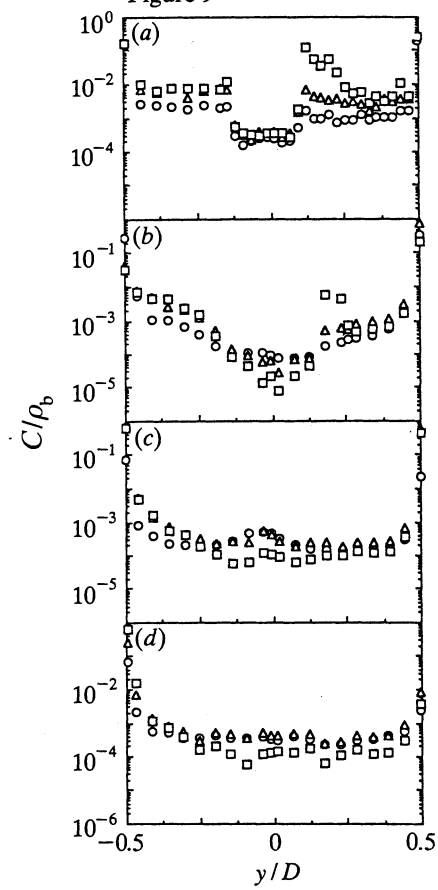

Figure 8. Radial profiles of concentration (C) in the sudden expansion ratio of 3.33 at z/D = (a) 0.3, (b) 3.2, (c) 4.4 and (d) 8 for 40 μm beads for mass loadings 13% (○), 40% (△) and 80% (□). Normalization is by the glass bead density ρ_b.

Figure 9. Radial profiles of concentration (C) in the sudden expansion ratio of 5 at z/D = (a) 0.08; (b) 1.33, (c) 2.67 and (d) 5.33 for 40 μm beads for mass loadings 13% (○), 40% (△) and 80% (□). Normalization is by the glass bead density ρ_b.

flow-rate, in contrast of the locus of the zero axial velocity. This is caused by the reduced response of the beads to the gas flow as the air flow-rate increased as explained in detail in §3d.

(c) *Influence of bead size and step height on bead dispersion*

Flow visualization showed that bead size and step height were important to bead dispersion and that a value of St_e of around unity led to an abrupt increase in dispersion. Detailed profiles of bead concentration for the two expansion ratios and two bead sizes are presented below and are used to quantify bead dispersion.

For the expansion ratio of 3.33, the 80 μm beads did not enter the recirculation zone and the concentration profiles resemble that of the jet flow of Hardalupas *et al.* (1989) and are not presented here. The radial concentration profiles of the 40 μm beads, figure 8, show a region of nearly constant concentration close to the step and inside the recirculation zone. These beads were dispersed backwards from the air

Table 7. *Normalization parameters and Stokes numbers in the expansion ratio of* 3.33
(Air flow-rate is 150 dm^3 min^{-1}.)

beads		U_0/(m s^{-1})	G_0/(kg m^{-2} s^{-1})	St_ω	St_{tr}	St_e
40 μm	13 %	1.19	0.19	7.4	1.9	1.2
	40 %	1.19	0.60	10.3	2.3	1.2
	80 %	1.19	1.16	13.7	2.7	1.2
80 μm	23 %	1.27	0.33	1.0	0.3	0.2
	40 %	1.27	0.59	1.3	0.4	0.2
	86 %	1.27	1.26	1.9	0.5	0.2

Table 8. *Normalization parameters and Stokes numbers in the expansion ratio of* 5
(Air flow-rate is 150 dm^3 min^{-1}.)

beads		U_0/(m s^{-1})	G_0/(kg m^{-1} s^{-1})	St_ω	St_{tr}	St_e
40 μm	13 %	0.57	0.09	9.9	3.3	4.4
	40 %	0.57	0.27	11.7	3.5	4.4
	80 %	0.57	0.52	14.4	4.1	4.4
80 μm	23 %	0.57	0.15	2.8	1.0	0.9
	40 %	0.57	0.26	3.1	1.0	0.9
	86 %	0.57	0.56	3.6	1.2	0.9

reattachment point and could not have entered the recirculation zone close to the step, since there is no time for them to respond to the gas flow. On the wall, however, the concentration is higher than in the rest of the recirculation zone by an order of magnitude and the large radial concentration gradient inside the recirculation zone downstream of the step was caused by the centrifuging of the beads on the wall. Bead dispersion is associated with the large eddies Stokes number, St_e, of the order of unity, as shown in tables 7 and 8, and the influence of the term $U_0/(U_0+U_{slip})$ on the estimates of St_e (equation (3)) was assumed negligible. In figure 8, the normalized bead concentration on the wall is in some regions close to one, which means that the beads were so highly concentrated that the volume fraction of glass approached 100 % with bead to bead interaction, as suggested by Lumley (1978). Downstream of the recirculation zone, the central maximum in the profile decays but, unsurprisingly, the near-wall maximum does not. The large inertia of the beads in conjunction with the decrease in eddy timescale associated with the split of the shear layer at reattachment (Bradshaw & Wong 1972), prevented any rapid dispersion of the curtain of beads away from the wall. The asymmetry of the concentration profiles for the higher mass loadings (40 % and 80 %), is caused by the attenuation of the incident laser beams by the beads, an effect known as turbidity.

For the expansion ratio of 5, the 80 μm beads enter the recirculation zone. The effect of the change of the step height on the timescale T_f of the large eddies (equation (2)) is given, for constant air flow-rate, by

$$\frac{T_{f1}}{T_{f2}} = \frac{h_1}{h_2}\left(\frac{h_1+\frac{1}{2}d}{h_2+\frac{1}{2}d}\right)^2, \tag{9}$$

where subscripts 1 and 2 refer to the previous and the new condition and d is the diameter of the upstream tube. The increase in expansion ratio leads to an increase in the timescale of the large eddies by a factor of around 3.5 and in an increase of the

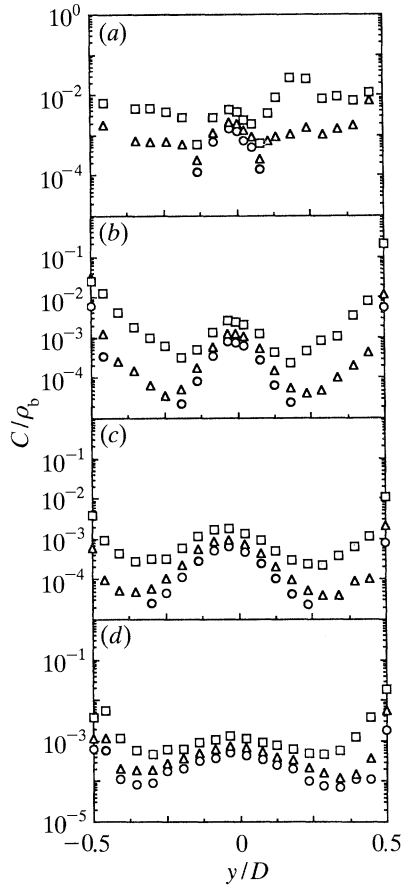

Figure 10. Radial profiles of concentration (C) in the sudden expansion ratio of 5 at z/D = (*a*) 0.08, (*b*) 1.33, (*c*) 2.67 and (*d*) 5.33 for 80 μm beads for mass loadings 23% (○), 40% (△) and 86% (□). Normalization is by the glass bead density ρ_b.

large eddies Stokes number for the 80 μm beads from 0.23 to around unity. The latter value confirms that the 80 μm beads could respond to the large eddies of the shear layer of the large expansion ratio and hence disperse inside the recirculation zone.

The radial profiles of concentration for the 40 μm and 80 μm beads in the expansion ratio of 5, figures 9 and 10 respectively, show that both bead sizes enter the recirculation zone and that their wall concentration is far larger than anywhere else inside the recirculation zone. The differences in bead concentration between the two bead diameters is small inside the recirculation zone, although the 80 μm beads have minimum concentration in the recirculation zone, in contrast to the constant concentration of the 40 μm beads there. The large eddies Stokes number of the 80 μm beads is around unity, so that they were centrifuged out of the large eddies more than the 40 μm beads, as argued by Crowe *et al.* (1985) and Kamalu *et al.* (1989), and resulted in the measured RMS of the fluctuations of the bead radial velocity (figure 17), being larger for the 80 μm than the 40 μm beads in certain regions of the flow. The increased dispersion of the 80 μm beads relative to the 40 μm beads resulted in similar concentrations of 40 μm and 80 μm beads in the recirculation zone, although the 40 μm beads remain longer in the large eddies of the shear layer because of their

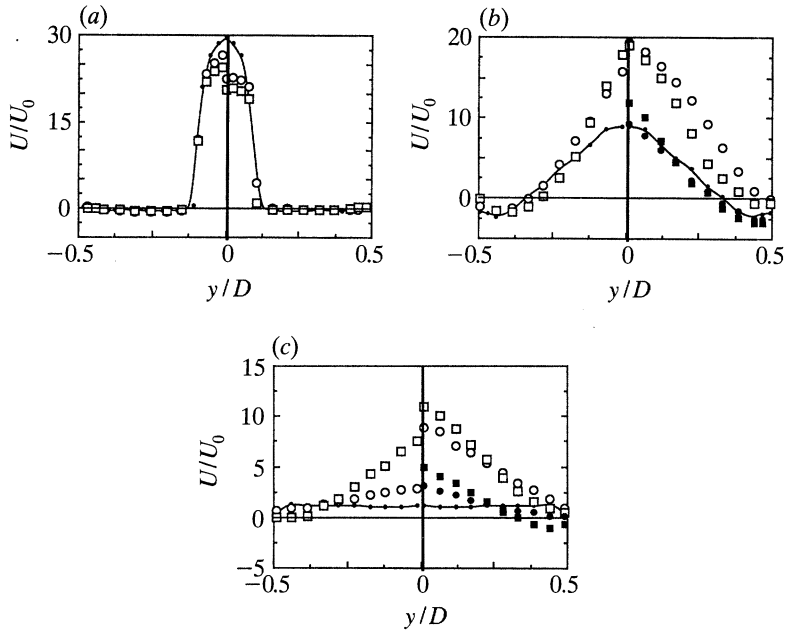

Figure 11. Radial profiles of mean axial velocity (U) in the sudden expansion ratio of 5 at (a) $z/D = 0.08$, (b) $z/D = 2.67$ and (c) $z/D = 5.33$. Left side of the figures corresponds to 40 μm beads for mass loadings 13 % (○) and 80 % (□) compared with the single phase (——). Right side of the figures corresponds to 80 μm beads for mass loadings 23 % (○) and 86 % (□) and the gas phase (23 % (●), 86 % (■)) in the presence of 80 μm beads compared with the single phase (——). Normalization is by the gas velocity, averaged over the area of the large tube, U_0.

larger St_e. The Stokes number of the 40 μm beads increased by a factor of 3.5 in the larger expansion ratio and resulted in more spatially uniform concentration profiles in the recirculation zone than in the small expansion ratio, but not in an increase in bead concentration. This confirms that the abrupt change of the bead concentration inside the recirculation zone occurs for St_e around unity and that an increase to 5 gives little further modification.

(*d*) *Influence of transit time across the reattachment length, mean flow centrifuging and gravity on bead dispersion*

This section demonstrates that the transit Stokes number, St_{tr}, and the centrifuge Stokes number, St_ω, must be larger than unity for the possible dispersion of the beads in the recirculation zone due to their response to the large eddies.

The radial profiles of axial mean velocity of the 40 μm and 80 μm beads in the expansion ratio of 5, figure 11, show that the beads leave the nozzle with a lower velocity than the gas phase, since they do not interact for long enough with the gas phase flow in the upstream tube to accelerate to the gas velocity by the time they reach the expansion. However, after a distance of $\frac{1}{2}D$ from the sudden expansion plane, the beads move faster than the gas phase, and so a slip velocity between the gas phase and the beads develops in the shear layer, which is larger for the 80 μm beads.

The mean transit time of the beads along the reattachment length was estimated by taking into account their deceleration on the centreline along the reattachment length, as suggested in §1 (equation (4)). The resulting value is the minimum

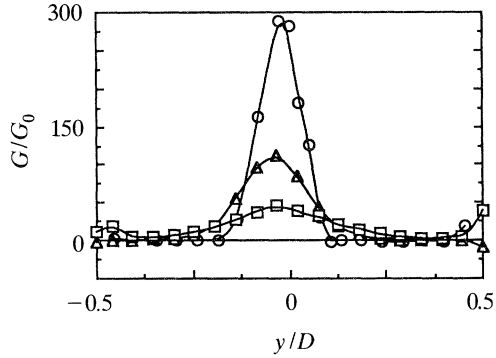

Figure 12. Radial profiles of axial flux of the 80 μm beads for mass loading of 40 % in the expansion ratio of 5 at $z/D = 0.08$, (○), 2.67 (△) and 5.33 (□). Normalization is by the flux, G_0, averaged over the area of the large tube.

transit time, since beads away from the centreline have lower velocities and longer transit times and can, as a consequence, be expected that a larger proportion of beads contributes to those which recirculate. The transit Stokes number, St_{tr}, is presented in tables 7 and 8. The 40 μm beads dispersed in the recirculation zone for both expansion ratios and the 80 μm only for the expansion ratio of 5 and St_{tr} was always unity or greater, confirming their ability to respond to the mean flow and eventually to the large eddies of the shear layer. In the smaller expansion ratio it was less than unity and the 80 μm beads did not disperse into the recirculation zone.

The centrifuge Stokes number, St_ω, is shown in tables 7 and 8 for the two expansion ratios. The radius of curvature of the separation streamline was estimated as the arc of a circle which was tangent to the upstream tube and passed through the reattachment point and the angular velocity, ω (equation (5)), was estimated from the radius of the circle and the inlet centreline velocity of the disperse phase. For the 40 μm beads, St_ω was of the order of 10 for the two expansion ratios and the influence of the centrifuging effect on their motion negligible. However, St_ω for the 80 μm beads was of the order of unity for the expansion ratio of 5 and mean flow centrifuging could affect their motion, so that they, like the 40 μm beads, should have longer reattachment lengths than the gas phase, so larger radius of curvature of the bead separation 'streakline'. However, figures 4 and 11 show that the 80 μm beads mean axial velocity is positive inside the mean gas phase recirculation zone of the expansion ratio of 5, implying shorter reattachment length than the gas phase. This result stemmed from the partial response of the beads to large eddies which caused high axial bead velocities to be present inside the gas phase recirculation zone and resulted to bimodal probability distribution function of the 80 μm beads (figure 14), with the high velocity part of the bimodal pdf corresponding to trajectories 1 of figure 1, and the low velocity peak associated with recirculating or nearly recirculating beads. The net consequence is that the arithmetic mean axial velocity was large and positive inside the gas phase recirculation zone and much different from the axial flux. Thus, the bead reattachment length should be defined in terms of the zero flux line, but figure 12 shows that the 80 μm beads axial flux is small but still positive in large parts of the gas phase recirculation zone.

The additional factor contributing to the above result, is the weight of the beads which in our flow acts in such a way that beads leave the recirculation zone and the net result is a bead reattachment length smaller than that of the air. Appendix B

evaluates the Froude number of the beads and the resulting estimates show that when the slip velocity between the 80 μm beads and the gas phase in the recirculation zone is less than around U_0, these move in the direction of gravity, and thus away from the recirculation zone. The comparative importance of weight is smaller, but not negligible, for the 40 μm beads and its principal effect is to make the beads leave the recirculation zone by sliding down the wall. The implication is that the beads would fall towards the step of the expansion and accumulate there, if the air flow was against the gravity vector.

The increase of the air flow-rate reduces the Stokes numbers of the mean flow parameters to unity or below (tables 5 and 6) and limits the dispersion of the 40 μm beads in the recirculation zone. Comparison between figures 5*a* and 6*a* shows that for a given value of the St_e, the concentration is different in the two expansion ratios. This is because bead dispersion is also influenced by the mean transit time, St_{tr} (equation (4)), which is different in the two expansion ratios. Although the recirculation zone is longer in absolute terms for the larger expansion, tables 5 and 6 show that St_{tr} is less favourable to bead dispersion (i.e. smaller) as the air flow-rate increases, because the transit time is shorter as the centreline mean axial velocity in figure 7 confirms. The centrifuge Stokes number, St_ω, decreased with the increase of air flowrate, but remained always larger than unity, contributing less than the transit time in the limitation of bead dispersion.

The mean velocity results of figure 11 can suggest the influence of the term $U_0/(U_0+U_{slip})$ of (3) on the estimates of the large eddies Stokes number, St_e, which was assumed negligible in the values of St_e presented in tables 7 and 8. The maximum value of slip velocity of the 40 μm beads in the shear layer of the expansion ratio of 5 is around $0.3U_0$ and so the effect of U_{slip} on the values of St_e is small. For the 80 μm beads, U_{slip} can be as large as $5U_0$ in the expansion ratio of 5 and can result in reduction of the values of St_e presented in table 8 by a factor of around 6 and hence partial response of the 80 μm beads to the large eddies and bimodal velocity probability distribution functions of §3*f*.

(*e*) *Influence of bead mass loading on bead dispersion*

The radial profiles of concentration of the 40 μm beads for mass loadings of 13%, 40% and 80%, figures 8 and 9 for the two expansion ratios, and of the 80 μm beads for mass loadings of 23%, 40% and 86% for the larger expansion ratio, figure 10, show that when the transit time Stokes number and the large eddies Stokes number are around unity, as for the 40 μm beads in the expansion ratio of 3.33 and for the 80 μm for the expansion ratio of 5, the bead dispersion inside the recirculation zone increases with the mass loading, while the effect is small for the 40 μm beads in the expansion ratio of 5 where the Stokes numbers are around 4 (figure 9). The increased dispersion is due to the increase of reattachment length of the gas phase flow with the mass loading shown in figures 3 and 4, which resulted in an increased mean transit time Stokes number and hence increased probability of the beads dispersing into the recirculation zone.

The central part of the gas phase flow in the presence of the 80 μm beads is accelerated with the increase of mass loading, figure 11, because of the transfer of momentum from the beads to the gas and the gas phase recirculation zone is extended. The transit Stokes number therefore also increases with mass loading (table 8) resulting in a larger bead concentration in the recirculation zone with the larger expansion ratio 5 (figure 10). With the small expansion ratio, the transit

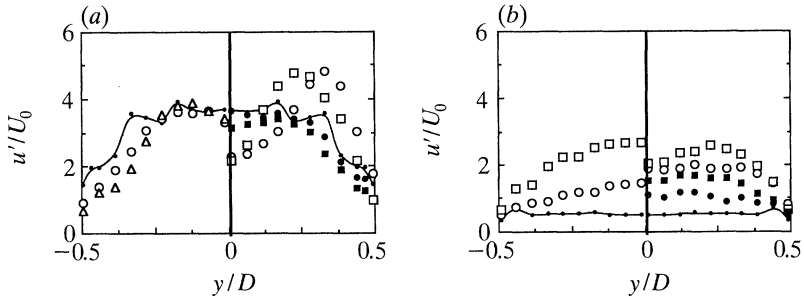

Figure 13. Radial profiles of RMS fluctuations of axial velocity (u') in sudden expansion ratio of 5 at (*a*) $z/D = 2.67$ and (*b*) $z/D = 5.33$. Left side of the figures corresponds to 40 μm beads for mass loadings 13% (○) and 80% (△) compared with the single phase (——). Right side of the figures corresponds to 80 μm beads for mass loadings 23% (○) and 86% (□) and the gas phase (23% (●), 86% (■)) in the presence of 80 μm beads compared with the single phase (——). Normalization is by the gas velocity, averaged over the area of the large tube, U_0.

Stokes number is always lower than unity (table 7) and, combined with the low large eddies Stokes number, prevented bead dispersion to the recirculation zone even for the highest mass loading.

The gas phase was not measured in the presence of the 40 μm beads, but the reattachment length of the beads was longer than that of the single phase and increased with mass loading (figures 3, 4 and 11). Since the drag force is the driving force for the bead movement backwards from the gas reattachment point inside the recirculation zone, it may be assumed that the gas phase recirculation was at least as long as that of the 40 μm beads. The implied lengthening of the gas phase recirculation zone caused the higher concentration of the 40 μm beads at the higher mass loadings in the expansion ratio of 3.33 and the change in St_{tr} (table 7) supports the argument. With the larger expansion ratio, the large eddies and the transit time Stokes number for the 40 μm beads were greater than unity, so that particle dispersion into the recirculation zone was large and independent of the reattachment length.

A possible explanation for the increase in bead dispersion with mass loading for the 80 μm beads in the larger expansion ratio, and for the 40 μm beads in the smaller expansion ratio, might be the modification of the gas phase turbulence in addition to the reasons considered in the previous paragraphs. The RMS axial velocity of the gas phase in the expansion ratio 5, figure 13, in the presence of the 80 μm beads is suppressed up to around 3*D* relative to that of the single phase, particularly inside the recirculation zone. This is inconsistent with the observed large bead dispersion. However, farther downstream, the fluctuations of the gas phase axial velocity are larger than those of the single phase and increase with bead loading. It is doubtful that the increase of gas phase turbulence could be held responsible for the larger bead dispersion of the higher mass loadings of the 80 μm beads in the expansion ratio of 5, since no comparable increase in the dispersion of the 40 μm beads in the expansion ratio of 5 was observed. The increased gas phase turbulence was due to the greater mean rate of strain in the gas mean flow, due to the momentum transfer from the beads. In the recirculation zone, the gas turbulence was suppressed even for the expansion ratio of 3.33, where no 80 μm beads were present inside the recirculation zone and arose from the modification of the mean gas phase flow field as a whole, figure 11, rather than through local changes of the gas phase turbulence. A similar

PHILOSOPHICAL TRANSACTIONS OF THE ROYAL SOCIETY A MATHEMATICAL, PHYSICAL & ENGINEERING SCIENCES

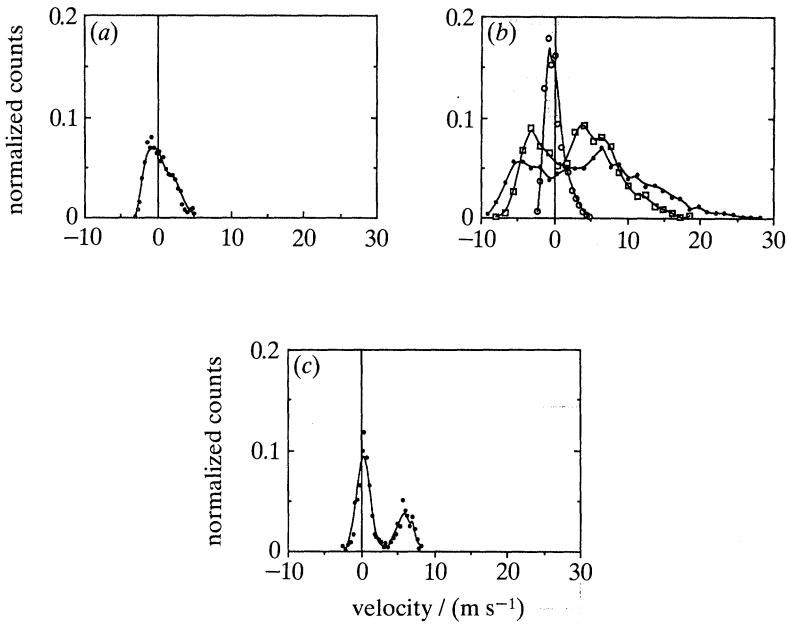

Figure 14. Axial velocity component (U) probability density functions in sudden-expansion ratio of 5 at $z/D = 1.33$ and $y/D = 0.25$ for: (*a*) the single phase when the air flow-rate was 150 dm^3 min^{-1}, (*b*) the 40 μm beads as a function of different large eddies Stokes number (0, 4.41; □, 1.68; ●, 1.26) modified by varying the air flow-rate (note that the large eddies Stokes number of 4.41 corresponds to air flow-rate of 150 dm^3 min^{-1}) and (*c*) the 80 μm beads for large eddies Stokes number of 0.9 corresponding to air flow-rate of 150 dm^3 min^{-1}.

effect on the gas phase turbulence inside a recirculation zone has been reported by Maeda *et al.* (1982) and in their case resulted in reduced heat transfer rates to the wall.

(*f*) *Bead motion due to large eddies*

The previous sections have shown that there is a strong correlation between bead dispersion into the recirculation zone and the large eddies of the shear layer, resulting in an abrupt change in bead dispersion for large eddies Stokes number around unity. However, it is not clear how the large eddies affect bead motion and the bead velocity measurements are examined here to indicate detailed characteristics of their motion. The results also show how examination of velocity characteristics in isolation can lead to wrong conclusions about bead dispersion.

The results of figure 14 show that the axial velocity probability distribution functions in the neighbourhood of the mean gas phase separation streamline are bimodal when the large eddies and the transit Stokes numbers of the beads are around unity. The axial velocity probability distribution function (PDF) of the 80 μm beads around the gas phase separation streamline in the expansion ratio of 5, e.g. at $z/D = 1.33$ and $y/D = 0.24$, shows that there are bead axial velocities present in the recirculation zone which are much larger than those of the single phase flow. The PDF of the 40 μm beads is not bimodal at the same air flow-rate and its width is smaller than that of the single phase, as expected for beads which acquire only a portion of the gas phase turbulence. However, the large eddies Stokes number of the 40 μm beads decreased to around unity, and their transit Stokes number to less than unity

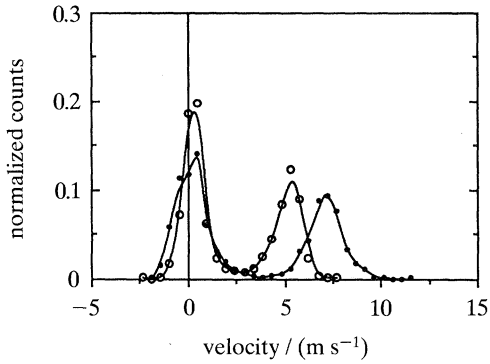

Figure 15. Probability density functions of the velocity components in directions inclined by $\pm 45°$ relative to the axis z of the expansion ($U_{+45°}$ (○), $U_{-45°}$ (●)) for the 80 μm beads in the sudden expansion ratio of 5 at $z/D = 2.67$ and $y/D = 0.19$.

with increase in air flow-rate so that the axial velocity PDF also became bimodal and similar to that of the 80 μm beads (figure 14*b*). The PDF of the bead radial velocity was also bimodal when the axial velocity PDF was bimodal and the region of bimodality extended from the wall to the centreline, particularly in the region close to reattachment. The bead velocity characteristics are explained as follows. The high axial velocity 80 μm beads acquire a radial velocity component by being centrifuged out of the large eddies of the gas flow and conserve this velocity component longer than the 40 μm beads, which follow the gas flow more faithfully but disperse less in the radial direction (Kamalu *et al.* 1989). The low axial velocity 80 μm beads are recirculating beads which entered the recirculation zone of the gas phase at an earlier instant. Similar reasons cause the bimodal axial velocity PDFs of the 40 μm beads at increased air flow-rates. So beads with relaxation time close to the timescale of the large eddies disperse faster than the gas phase and other beads in the cross stream direction and the same result was predicted by Chung & Troutt (1988) and Chein & Chung (1987).

The probability distribution functions of the velocity components in directions inclined at $\pm 45°$ relative to the tube axis of the 80 μm beads around the gas separation streamline in the expansion ratio of 5, for example at $z/D = 0.67$ and $y/D = 0.19$ (figure 15), are also bimodal. The peak around zero velocity corresponds to the recirculating beads and the figure implies that no preferred trajectory angle is associated with these velocities. The other peak corresponds to beads with large axial and large radial velocities towards the tube wall which have a mean trajectory angle around 9° to the z coordinate direction at $y/D = 0.19$, estimated from the velocity difference between the high velocity peaks in the two directions. The rms trajectory angle of the beads at the exit of the jet, estimated locally by $\arctan[v'_b(r)/U_b(r)]$ from the measured velocities, is approximately $\pm 3°$. So the high velocity beads inside the gas recirculation zone can only come from the free stream after their partial interaction with the large eddies of the shear layer and not because of their initial trajectories or the mean gas flow field, since a bead mean trajectory with angle of 9° at $y/D = 0.19$ crosses the gas separation streamline. The bead cross-correlation coefficient, $\overline{u_b v_b}/u'_b v'_b$, for the 40 μm and 80 μm beads, (figure 16) is larger than that of the gas phase which is expected to be around 0.6 in the shear layer (Etheridge & Kemp 1978). The correlation coefficient of the 40 μm beads is around 0.8 and of the 80 μm beads around 1 and such high values are caused by deterministic bead

PHILOSOPHICAL TRANSACTIONS OF THE ROYAL SOCIETY A MATHEMATICAL, PHYSICAL & ENGINEERING SCIENCES

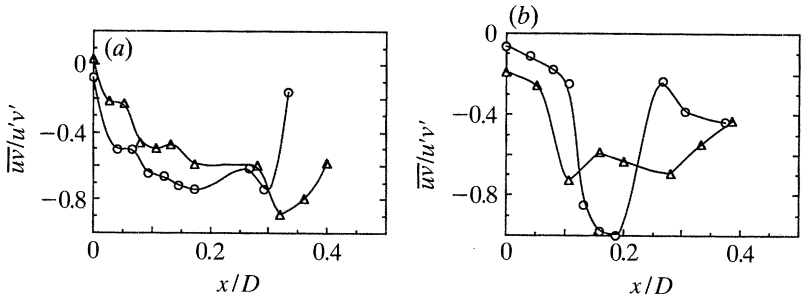

Figure 16. Radial profiles of the correlation coefficient $\overline{uv}/u'v'$ in the sudden expansion ratio of 5 at $z/D = 0.67$ (○) and 2.67 (△) for (*a*) 40 μm beads for mass loading of 13% and (*b*) 80 μm beads for mass loading of 86%.

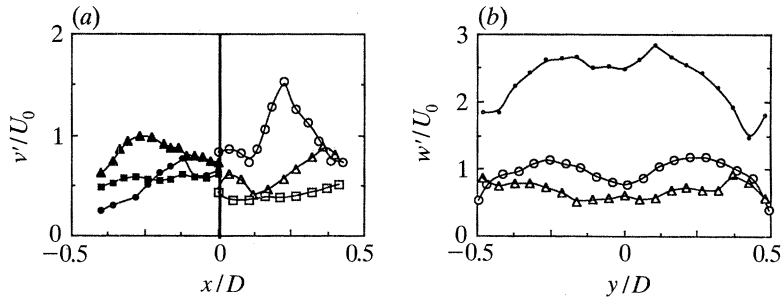

Figure 17. (*a*) Radial profiles of RMS fluctuations of the radial velocity (v') in sudden expansion ratio of 5 at $z/D = 0.67$ (○), 2.67 (△) and 5.33 (□) for the 40 μm beads for mass loadings 13% (left side) and the 80 μm beads for mass loading of 86% (right side). (*b*) Radial profiles of RMS fluctuations of azimuthal velocity (w') in sudden-expansion ratio of 5 at $z/D = 2.67$ for 40 μm beads for mass loading of 13% (○) and for 80 μm beads for mass loading of 86% (△) compared with the single phase (——). Normalization is by the gas velocity, averaged over the area of the large tube, U_0.

trajectories like those of Hardalupas *et al.* (1989). This is true for bead trajectories entering the recirculation zone with large axial velocities as shown by the PDF of figure 15.

The response of the beads to the large eddies affects the RMS of the fluctuations of their axial and radial velocities and when the large eddies and the mean transit time Stokes numbers are around unity, the following were found. The RMS of the fluctuations of the 80 μm beads axial and radial velocities, u'_b and v'_b, are larger than those of the 40 μm beads which have larger Stokes numbers (figures 13 and 17*a*), implying better response of the 80 μm beads to the gas phase flow. Also, u'_b is larger than that of the gas phase (figure 13) in certain regions of the flow. These results imply that the beads disperse radially more than the gas phase, that the 80 μm beads disperse more than the 40 μm beads and that the 40 μm beads disperse more at higher air flow-rate. However, the concentration measurements of figures 5, 6, 8, 9 and 10 show the opposite, despite the relative magnitude of the turbulent velocities. So the partial response of the beads to the large eddies of the shear layer limits the number of beads dispersed into the recirculation zone, but those captured by the large eddies are dispersed in such a way that results in large RMS fluctuations of the velocity components.

The locus of maximum v'_b of the 40 μm beads occurred on the near wall side of the separation streamline downstream from the inlet pipe (figure 17*a*), in contrast to that of the axial velocity RMS fluctuations (figure 13), which occurred always at around

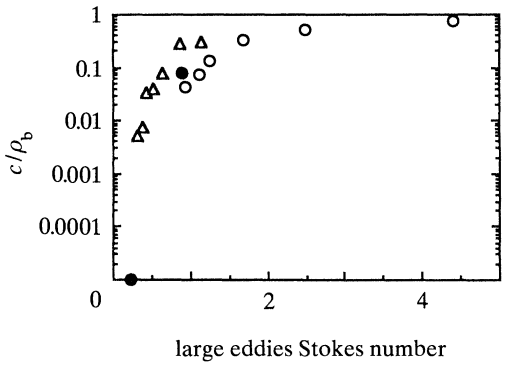

Figure 18. Experimentally obtained relationship between large eddies Stokes number, St_e, and bead concentration (C) inside the recirculation zone, approximated here with the integral of the bead concentration on the wall. The measurements for 40 μm (○, △) and 80 μm (●) beads and the expansion ratios of 3.33 and 5 are considered.

$|y/D| = 0.2$. This characteristic of the 40 μm bead axial and radial velocity RMS fluctuations has also been observed in single phase flows (Etheridge & Kemp 1978; Bradshaw & Wong 1972) and this similarity suggested good response of the beads to the gas turbulence. However, there was a large anisotropy between v'_b and u'_b in the shear layer ($u'_b \approx 5v'_b$) while in the single phase flow v'_s was only around 2 times smaller than u'_s (Etheridge & Kemp 1978). The bead turbulence anisotropy and the high bead correlation coefficient are characteristic of the fan spreading mechanism (Hardalupas *et al.* 1989), whereby the superposition of trajectories from different regions of the flow lead to large bead RMS fluctuations. It is likely that fan-spreading, because of the recirculation zone and associated streamline curvature, is an important contributor to bead axial and radial RMS fluctuations.

The RMS values of the azimuthal velocity, w'_b (figure 17*b*), do not have bimodal PDFS as the other two components do and w'_b of the 80 μm is lower than that of the 40 μm beads. The fan-spreading effect of the large eddies cannot have any effect on the azimuthal direction and it is the only RMS component indicating smaller response of the 80 μm beads to the gas turbulence than that of the 40 μm beads, so it can be argued that w'_b is a measurement of the response of the beads to the gas turbulence. The difference in w'_b between the 80 μm and 40 μm beads is, however, only 10%, smaller than might be expected from the ratio of their relaxation times, a factor of 4, and indicates the amount of turbulence energy existing in the timescales of the spectrum where the 40 μm beads respond additionally to those of the 80 μm. For the 40 μm beads w'_b is smaller than that of the single phase by a factor of around 2.5, which suggests that they acquire about 40% of the gas turbulence.

4. Discussion

One of the aims has been to quantify bead dispersion in the recirculation zone and establish the contribution of different parameters. The bead concentration inside the recirculation zone correlates with the large eddies Stokes number and figure 18 shows that for values of St_e of the order of unity there is an abrupt change in bead dispersion after which there is little change up to the examined St_e value of 5. However, the transit time Stokes number, St_{tr}, and the centrifuge Stokes number, St_ω, are also controlling parameters and both should be larger than unity to allow

interaction with the large eddies. The transit time and the centrifuge Stokes numbers and the large eddies Stokes number are independent parameters in some practical applications and, for example, the injection velocity of droplets in a liquid fuel burner can be varied independently of the turbulent timescale of the flow, which is defined by the geometry of the burner and the velocity of the combusting air. So bead sizes for which St_e is around unity can be prevented from entering the recirculation zone if their transit time across the length of the recirculation zone is too short, leading to St_{tr} less than unity. This effect is important for the larger droplets in the spray, which usually carry most of the fuel flow-rate, because their response time allows them to respond only to the largest eddies of the flow.

When $St_{tr} > 1$ and $St_\omega > 1$, then the following parameters may still affect bead dispersion in the recirculation zone, even when St_e is around unity. First, the slip velocity of the beads tends to increase the apparent frequency of the large eddies as noted by Hishida *et al.* (1989) and Squires & Eaton (1990) in a different context and decreases bead response to the large eddies as equation (A1) in Appendix A quantifies. Second, bead weight can affect bead dispersion, when their velocity is small as quantified in Appendix B and depending on the direction of gravity relative to the flow can either enhance or limit dispersion. In our experiment bead weight resulted in removing the beads from the recirculation zone, since the mean flow there was opposite to the direction of gravity, while in the horizontal backward facing step of Ruck & Makiola (1988), weight was responsible for beads entering the recirculation zone.

The locations and rate at which the discrete phase enters or leaves the recirculation zone are important for combustion applications, since these regions can affect the local air to fuel ratio and result in rich or lean conditions. Entry into the recirculation zone occurred close to the reattachment region, where the lengthscale of the large eddies in the shear layer was of the order of the step height and the discrete phase reached the wall either with large axial velocities, when their initial velocity was large or, they were centrifuged by the large eddies to the wall when their initial velocity was small. Exit from the recirculation zone occurred either at the reattachment point, due to the weight of the discrete phase, or near the step due to interaction with large eddies. The beads, when inside the recirculation zone, moved backwards, when the backward gas flow motion had enough momentum to overcome the weight of the beads, and fell due to gravity when it did not.

The abrupt change of bead dispersion for large eddies Stokes number around unity of our experiment is in agreement with others in the literature. Humphries & Vincent (1978) found that for $St_e \approx 1$ particle dispersion increased leading to decreased particle residence time inside the recirculation zone and the calculations of Chein & Chung (1987) and the experiments of Kamalu *et al.* (1989) suggested that this occurred due to centrifuging by the large eddies. The effect of the large eddies on bead motion resulted in bimodal probability distribution function of the axial and radial bead velocity in the neighbourhood of the mean gas separation streamline, large bead anisotropy and high bead cross-correlation coefficient which are in agreement with the fan-spreading mechanism of the bead motion of Hardalupas *et al.* (1989). The centrifuging of the beads by the large eddies from high to low velocity regions of the shear layer resulted in a net bead flux towards the recirculation zone, so asymmetric dispersion of the beads, which does not happen in the gas phase flow and has also been observed in the disperse phase of the plane mixing layer experiments of Kobayashi *et al.* (1988) and Hishida *et al.* (1989). It is therefore

important that mathematical models of turbulent particle dispersion, such as that of Gosman & Ioannides (1983), should include the centrifuging effect due to the vorticity of the large eddies.

The timescale of the large eddies was estimated by analogy with a plane mixing layer, although preferred frequencies in turbulent recirculation bubbles have been found by Gutmark & Ho (1983) and Kiya & Sasaki (1985) to compare with $f_i = 0.5\, U_i/d$, where U_i and d are the area average velocity and the diameter of the upstream pipe, and $f_i = 0.65\, U_\infty/Z_r$, where U_∞ is the free stream velocity and Z_r the reattachment length respectively. The former implies timescales of 5 ms independent of expansion ratio, and the latter 20 ms for the expansion ratio of 3.33 and 35 ms for the expansion ratio of 5, so there are low frequency eddies with enough energy content to disperse the beads. It should be noted that the lengthscale of the gas recirculation zone increases proportionally to the step height, but the reverse gas phase velocity, responsible for the backward motion of the beads from the reattachment point inside the recirculation zone, is inversely proportional to the step height, so that it should lead to decreased bead dispersion after a certain step height.

The central part of the gas flow accelerated relative to the single phase flow due to the transfer of bead momentum flux, in agreement with the jet results of Hardalupas *et al.* (1989). As a consequence of mass conservation, lower gas velocities existed close to the wall and lead to an increase in gas flow reattachment length with increase in mass loading. In turn, the increased reattachment length allowed more beads to disperse in the recirculation zone at the higher mass loadings.

The gas turbulence was reduced relative to the single phase flow close to the inlet and inside the recirculation zone and increased downstream of the reverse flow region close to the wall, but the magnitude of the modification was too small to affect dispersion. There are five candidate mechanisms to explain the gas phase modification. The first, suggested by Pismen & Nir (1978), shows that the maximum dissipation rate of turbulence per unit bead mass is achieved for beads with relaxation times of the same order of magnitude as the characteristic turbulence timescale corresponding to intermediate wavenumbers of the turbulence spectrum and this parameter is similar to the large eddies Stokes number, St_e. The second mechanism is that the turbulence intensity of the gas in the presence of the beads is suppressed because the beads attenuate the high frequency fluctuations of the turbulence spectrum while the energy contained in the low frequency eddies is not affected (Al Taweel & Landau 1977; Owen 1969; Squires & Eaton 1990). However, this mechanism cannot explain the increased gas turbulence measured downstream of the recirculation zone. The third suggestion, to account for an increase in the gas turbulence, is the wakes shed by the beads due to the mean slip velocity between the two phases. It is doubtful whether this is sufficient since the slip Reynolds number was about 20 and hence well below the value of 44, at which the wake behind a sphere becomes unsteady. However, a referee suggested that the local fluctuations of the slip velocity could result in slip Reynolds number larger than 44 and increase the gas phase turbulence. Furthermore, the scale of the wake is of the order of a bead diameter and hence close to the Kolmogorov microscale, rather than near the energy containing scales as would be necessary for the increase of the gas turbulence. The fourth suggestion (Gore & Crowe 1989) correlates measurements of the gas phase turbulence modification with the ratio d_b/l_e, which appears in the definition of the large eddies Stokes number (equation (3)), with the only difference that l_e here is the lengthscale of the energy containing eddies and d_b is the bead diameter, and found

PHILOSOPHICAL TRANSACTIONS OF THE ROYAL SOCIETY A MATHEMATICAL, PHYSICAL & ENGINEERING SCIENCES

that gas turbulence is suppressed for values of $d_b/l_e < 0.1$ and increased for values larger than 0.1. The lengthscale of the energy containing eddies in our flow is around 10 times smaller than the lengthscale of the large eddies as argued in the introduction, resulting in ratios $d_b/l_e \approx 0.03$, suggesting suppression of turbulence. The fifth and more likely suggestion is that the increase in u_f' is due to generation of $\overline{u_f^2}$ by $[\overline{u_f v_f}\partial U_f/\partial y]$, which is larger due to the increase in the value of mean rate of strain, $\partial U_f/\partial y$ as the fluid is accelerated by the momentum transfered from the beads (Hardalupas *et al.* 1989). The reduced turbulence relative to the single phase flow in the recirculation zone arose also from the modification of the mean gas phase flow field as a whole, rather than through local changes of the gas phase turbulence.

This work was supported by the CEGB and the SERC through cofunded grant GR/C/47311 and by the Commission of the European Communities through the Non-Nuclear Energy R&D programme by contract EN3F-0022-GR. We thank Dr J. Gibb, of CEGB, Marchwood Engineering Laboratories, for many stimulating discussions. Mr J. R. Laker designed the zero-crossing phase-Doppler counter and Mr P. Trowell constructed the flow circuit and the receiving optics of the phase Doppler anemometer. A.M.K.P.T. was supported through the award of a Royal Society University Research Fellowship.

Appendix A. Large eddies Stokes number

Consider large eddies of lengthscale λ and convection velocity U_c, so the corresponding timescale is $T_f = \lambda/U_c$. Generally the particles may have a relative velocity, U_{slip}, to the convection velocity U_c of the large eddies. When the particles are moving faster than the eddies by U_{slip}, then the timescale of the large eddies is reduced and the large eddies Stokes number, St_e, is defined as

$$St_e = \frac{T_f}{\tau_b}\frac{U_c}{U_c + U_{slip}}. \tag{A 1}$$

For the Stokes régime $\tau_b = \rho_b d_b^2/18\mu_f$, so

$$St_e = \frac{\lambda/U_c}{\rho_b d_b^2/18\mu_f}\frac{U_c}{U_c + U_{slip}}. \tag{A 2}$$

It should be noted that the assumption of a Stokes régime in the calculation of the particle relaxation number, τ_b, results in underestimation of the Stokes number by a factor of $1 + 0.15Re_b^{\frac{2}{3}}$ (Clift *et al.* 1978), where $Re_b = U_{slip}\, d_b/\nu_f$ is the bead Reynolds number. However, the case examined here is the worst case, because large Stokes numbers imply better response to the gas flow. Then the Stokes number, St_e, can be expressed as a function of the flow Reynolds number based on the lengthscale of the large eddies and their convection velocity, $Re_\lambda = U_c\,\lambda/\nu_f$, as

$$St_e = 18\frac{\rho_f}{\rho_b}\left(\frac{\lambda}{d_b}\right)^2\frac{1}{Re_\lambda}\frac{U_c}{U_c + U_{slip}}, \tag{A 3}$$

where ρ_f and ρ_b the densities of the fluid and the beads respectively and d_b the diameter of the beads.

The large eddies Stokes number, St_e, in the shear layer of the sudden expansion flows can be estimated using (A 3) assuming that the lengthscale of the large eddies is the expansion step height, h, their convection velocity is the velocity of the fluid averaged over the area of the large tube, U_0, and the corresponding Reynolds number of the fluid is $Re_h = U_0 h/\nu_f$.

Table 9.

slip velocity, $U_{slip}/(m\ s^{-1})$	bead Froude number, Fr 40 μm	80 μm
2	23.9	7.1
1	10.5	2.9
0.5	4.8	1.3
0.1	0.9	0.2

Appendix B. Effect of bead weight on bead motion in the recirculation zone

The importance of the gravitational forces on the behaviour of the beads in the recirculation zone can be evaluated by assuming that the only forces acting on a single bead are drag and gravity. The drag force pushes the bead towards the step if it is larger than the gravitational force for the vertical flow arrangement. The bead equation of motion is thus

$$\rho_b(\tfrac{1}{6}\pi d_b^3)\frac{dU_b}{dt} = \tfrac{1}{2}\rho_f U_{slip}^2 C_D(\tfrac{1}{4}\pi d_b^2) - \rho_b(\tfrac{1}{6}\pi d_b^3) g, \tag{B 1}$$

where ρ_b and ρ_f are the density of the beads and the air respectively, d_b is the bead diameter, g is the acceleration due to gravity, U_{slip} is the slip velocity between the bead and the air and C_D is the drag coefficient. Equation (B 1) can be rewritten as

$$\frac{1}{g}\frac{dU_b}{dt} = \frac{3\rho_f C_D}{4\rho_b}\frac{U_{slip}^2}{d_b g} - 1. \tag{B 2}$$

The first term in equation (B 2) defines the dimensionless number

$$Fr = \frac{3\rho_f C_D}{4\rho_b}\frac{U_{slip}^2}{d_b g}, \tag{B 3}$$

which is a modified Froude number quantifying the influence of gravity on the behaviour of a single bead in a fluid flow. When $Fr > 10$, the drag force dominates and if $Fr < 10$ gravity dominates. However, if Fr is of the order of 1 the contribution of both forces is important.

The drag coefficient, C_D, is defined as a function of the bead Reynolds number, $Re_b = U_{slip} d_b/\nu_f$ (Clift *et al.* 1978),

$$C_D = \begin{cases} (24/Re_b)(1 + 0.15 Re_b^{\frac{2}{3}}) & \text{if } Re_b < 1000, \\ 0.44 & \text{if } Re_b > 1000. \end{cases} \tag{B 4}$$

By using the above equations the dimensionless number Fr is estimated for the 40 μm and 80 μm beads for different slip velocity in table 9.

Therefore the 80 μm beads in the recirculation zone are affected by gravity over a wide range of slip velocities. The 40 μm beads are affected by gravity only for small slip velocities.

References

Abbott, D. E. & Kline, S. J. 1962 Experimental investigation of subsonic turbulent flow over single and double backward facing steps. *J. Basic Eng* **84**, 317–325.

Al Taweel, A. M. & Landau, J. 1977 Turbulence modulation in two-phase jets. *Int. J. Multiphase Flow* **3**, 341–351.

Armaly, B. F., Durst, F., Pereira, J. C. F. & Schonung, B. 1983 Experimental and theoretical investigation of backward-facing step flow. *J. Fluid Mech.* **127**, 473–496.

Bradshaw, P., Ferris, D. H. & Johnson, R. F. 1964 Turbulence in the noise-producing region of a circular jet. *J. Fluid Mech.* **19**, 591–624.

Bradshaw, P. & Wong, F. Y. F. 1972 The reattachment and relaxation of a turbulent shear layer. *J. Fluid Mech.* **52**, 113–135.

Chein, R. & Chung, J. N. 1987 Effects of vortex pairing on particle dispersion in turbulent shear flow. *Int. J. Multiphase Flow* **13**, 785–802.

Cherdron, W., Durst, F. & Whitelaw, J. H. 1978 Asymmetric flows and instabilities in symmetric ducts with sudden expansions. *J. Fluid Mech.* **84**, 13–31.

Cherry, N. J., Hillier, R. & Latour, M. E. M. P. 1984 Unsteady measurements in a separated and reattaching flow. *J. Fluid Mech.* **144**, 13–46.

Chung, J. N. & Troutt, T. R. 1988 Simulation of particle dispersion in an axisymmetric jet. *J. Fluid Mech.* **186**, 199–222.

Clift, R., Grace, J. R. & Weber, M. E. 1978 *Bubbles, drops and particles*. London: Academic Press.

Crowe, C. T., Gore, R. A. & Troutt, T. R. 1985 Particle dispersion by coherent structures in free shear flows. *Particulate Sci. Technol.* **3**, 149–158.

Dodge, L. G., Rhodes, D. J. & Reitz, R. D. 1987 Drop-size measurement techniques for sprays: comparison of Malvern laser-diffraction and Aerometrics phase/Doppler. *Appl. Optics* **26**, 2144–2154.

Dring, R. P. & Suo, M. 1978 Particle trajectories in swirling flows. *J. Energy* **2**, 232–237.

Eaton, J. K. & Johnston, J. P. 1981 A review of subsonic turbulent flow reattachment. *AIAA J.* **19**, 1093–1100.

Etheridge, D. W. & Kemp, P. H. 1978 Measurements of turbulent flow downstream of a rearward-facing step. *J. Fluid Mech.* **86**, 545–566.

Fuchs, N. A. 1964 *The mechanics of aerosols*. Oxford: Pergamon Press.

Glass, M. & Kennedy, I. M. 1977 An improved seeding method for high temperature laser Doppler velocimetry. *Combust. Flame* **29**, 333–335.

Gore, R. A. & Crowe, C. T. 1989 Effect of particle size on modulating turbulent intensity. *Int. J. Multiphase Flow* **15**, 279–285.

Gosman, A. D. & Ioannides, E. 1983 Aspects of computer simulation of liquid fueled combustors. *AIAA J. Energy* **7**, 482–490.

Gould, R. D., Stevenson, W. H. & Thompson, H. D. 1990 Investigation of turbulent transport in an axisymmetric sudden expansion. *AIAA J.* **28**, 276–283.

Gutmark, E. & Ho, C. M. 1983 On the preferred modes and spreading rates of jets. *Phys. Fluids* **26**, 2932–2938.

Hardalupas, Y. 1989 Experiments with isothermal two-phase flows. Ph.D. thesis, University of London.

Hardalupas, Y. & Taylor, A. M. K. P. 1989 On the measurement of particle concentration near a stagnation point. *Exp. Fluids* **8**, 113–118.

Hardalupas, Y., Taylor, A. M. K. P. & Whitelaw, J. H. 1986 Two phase annular flow. In *Proc. 9th Australasian Fluid Mech. Conf.* pp. 238–242, Auckland, New Zealand.

Hardalupas, Y., Taylor, A. M. K. P. & Whitelaw, J. H. 1988 Measurements in heavily-laden dusty jets with phase-Doppler anemometry. In *Transport phenomena in turbulent flows: theory, experiment and numerical simulation* (ed. M. Hirata & N. Kasagi), pp. 821–835. Washington, D.C.: Hemisphere.

Hardalupas, Y., Taylor, A. M. K. P. & Whitelaw, J. H. 1989 Velocity and particle flux characteristics of turbulent particle-laden jets. *Proc. R. Soc. Lond.* A **426**, 31–78.

Hardalupas, Y., Taylor, A. M. K. P. & Whitelaw, J. H. 1990 Velocity and size characteristics of liquid-fuelled flames stabilised by a swirl burner. *Proc. R. Soc. Lond.* A **428**, 129–155.

Hardalupas, Y., Taylor, A. M. K. P. & Whitelaw, J. H. 1991 In *Applications of laser techniques to fluid mechanics* (ed. R. J. Adrian, D. F. G. Durão, F. Durst, M. Maeda & J. H. Whitelaw), pp. 183–202. Berlin: Springer-Verlag.

Hishida, K., Ando, A., Hayakawa, A. & Maeda, M. 1989 In *Applications of laser anemometry to*

PHILOSOPHICAL TRANSACTIONS OF THE ROYAL SOCIETY A MATHEMATICAL, PHYSICAL & ENGINEERING SCIENCES

fluid mechanics (ed. R. J. Adrian, T. Asanuma, D. F. G. Durão, F. Durst & J. H. Whitelaw), pp. 189–205.

Humphries, W. & Vincent, J. H. 1976 An experimental investigation of the detention of airborne smoke in the wake bubble behind a disk. *J. Fluid Mech.* **73**, 453–464.

Humphries, W. & Vincent, J. H. 1978 The transport of airborne dusts in the near wakes of bluff bodies. *Chem. Engng Sci.* **33**, 1141–1146.

Kamalu, N., Tang, L., Troutt, T. R., Chung, J. N. & Crowe, C. T. 1989 Particle dispersion in developing shear layers. In *Proc. Int. Conf. on Mechanics of Two-Phase Flows* (ed. Lee, S. L. and Durst, F.), pp. 199–202, Taipei, Taiwan: National Taiwan University.

Kiya, M. & Sasaki, K. 1985 Structures of large-scale vortices and unsteady reverse flow in the reattaching zone of a turbulent separation bubble. *J. Fluid Mech.* **154**, 463–491.

Khezzar, L., Whitelaw, J. H. & Yianneskis, M. 1986 Round sudden-expansion flows. *Proc. Instn. Mech. Engrs* **200**, 447–455.

Kobayashi, H., Masutani, S. M., Azuhata, S., Arashi, N. & Hishinuma, Y. 1988 Dispersed phase transport in a plane mixing layer. In *Transport phenomena in turbulent flows – theory, experiment and numerical simulation* (ed. M. Hirata & N. Kasagi), pp. 433–466. Washington, D.C.: Hemisphere.

Kriebel, A. R. 1961 Particle trajectories in a gas centrifuge. *J. Basic Engng* **83**, 333–340.

Lazaro, B. J. & Lasheras, J. C. 1989 Particle dispersion in a turbulent, plane, free shear layer. *Phys. Fluids* A **1**, 1035–1044.

Li, X. & Tankin, R. S. 1989 Spray behaviour in annular air streams. *Combust. Sci. Technol.* **64**, 141–165.

Lumley, J. L. (1978) Two phase and non-newtonian flows. In *Turbulence* (ed. P. Bradshaw), pp. 289–324, 2nd edn. Berlin: Springer-Verlag.

Maeda, M., Kiyota, H. & Hishida K. 1982 Heat transfer to gas-solids two-phase flow in separated, reattached and redevelopment regions. In *Proc. Seventh Int. Heat Transfer Conf.* (ed. U. Grigull, E. Hahne, K. Stephan & J. Straub), Hemisphere.

McDonell, V. G., Wood, C. P. & Samuelsen, G. S. 1986 A comparison of spatially resolved drop size and drop velocity measurements in an isothermal chamber and a swirl-stabilised combustor. In *Proc. 21st Symp. (Int.) on Combustion*, 685–694. Pittsburgh: The Combustion Institute.

Melling, A. & Whitelaw, J. H. 1975 Turbulent flow in a rectangular duct. *J. Fluid Mech.* **78**, 289–315.

Mostafa, A. A., Mongia, H. C., McDonell, V. G. & Samuelsen, G. S. 1987 On the evolution of particle-laden jet flows: a theoretical and experimental study. *AIAA paper no.* 87-2181.

Owen, P. R. 1969 Pneumatic Transport. *J. Fluid Mech.* **39**, 407–432.

Pismen, L. M. & Nir, A. 1978 On the motion of suspended particles in stationary homogeneous turbulence. *J. Fluid Mech.* **84**, 193–206.

Ruck, B. & Makiola, B. 1988 Particle dispersion in a single-sided backward-facing step flow. *Int. J. Multiphase Flow* **14**, 787–800.

Saffman, M. 1987 Automatic calibration of LDA measurement volume size. *Appl. Optics* **26**, 2592–2597.

Squires, K. D. & Eaton, J. K. 1990 Particle response and turbulence modification in isotropic turbulence. *Phys. Fluids* A **2**, 1191–1203.

Tennekes, H. & Lumley, J. L. 1972 *A first course in turbulence*. The MIT Press.

Thomas, N. H., Auton, T. R., Sene, K. & Hunt, J. C. R. 1983 Entrapment and transport of bubbles by transient large eddies in multiphase turbulent shear flows. In *Proc. Int. Conf. on the Physical Modelling of Multi-Phase Flow*, pp. 169–184.

Yanta, W. J. & Smith, R. A. 1978 Measurements of turbulence-transport quantities with a laser-Doppler velocimeter. *AIAA paper no.* 73-169.

Yuu, S., Yasukouchi, N., Hirosawa, Y. & Jotaki, T. 1978 Particle turbulent diffusion in a dust laden round jet. *A.I.Ch.E. J.* **24**, 509–519.

Received 28 January 1991; revised 17 February 1992; accepted 7 April 1992

PHILOSOPHICAL TRANSACTIONS OF THE ROYAL SOCIETY A MATHEMATICAL, PHYSICAL & ENGINEERING SCIENCES